

# Analysis of Leakage Cause of L415M Spiral Submerged Arc Welding Pipe

Yan Xu\*, Yinglai Liu, Xianghui Nie, Zhenjun Feng, Liang Li, Fengping Yang

Tubular Goods Research Center of CNPC, Xi'an, Shaanxi, 710077, China

**Abstract.** The causes of longitudinal crack in gas pipeline during pressure were analyzed by means of mechanical property test, microstructure analysis, sem analysis and energy spectrum analysis. The results show that the leakage of L415M spiral submerged arc welded pipe is caused by the contact between the base material of steel pipe and low-melting copper alloy in the process of high temperature, resulting in the brittleness of liquid metal. Specifically, when the leakage site of the steel pipe is heated at an abnormal high temperature, copper penetration along the grain boundary causes embrittlement, strength reduction and crack along the grain boundary, finally leading to the crack and leak of the steel pipe.

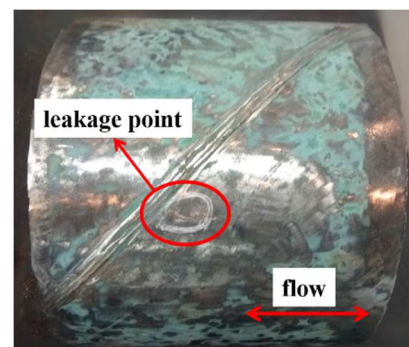
## 1 Introduction

The failure of product parts caused by liquid metal is a common problem in the current engineering production process. This brittle fracture often occurs in an instant, and the consequences are also very serious [1–2]. As the carrier of oil and gas transportation, steel pipes need to have excellent mechanical properties, because once accidents occur, the consequences will be disastrous [3–6]. Under certain temperature and tensile stress, the low melting point metal penetrates into the material from the surface of the part along the grain boundary, causing the embrittlement of the metal material and leads to the failure of the part. It is called the low melting point metal contact embrittlement crack, which is referred to as the metal erosion embrittlement crack or the low melting point metal thermal pollution crack. The design pressure of a gas pipeline is 6.3MPa. When the pressure rises to 1.25 times the design pressure during the hydraulic strength test of the process pipeline system in the construction unit, it is found that the pressure drops slowly at 0.1MPa per hour. The operator organizes personnel to patrol and find that the leakage point is 18.4km from the upstream station, which is located in the straight section and the buried depth of the pipeline is about 2.3 meters. The leakage pipe is  $\Phi 508\text{mm} \times 7.1\text{mm}$  L415M spiral submerged arc welded pipe.

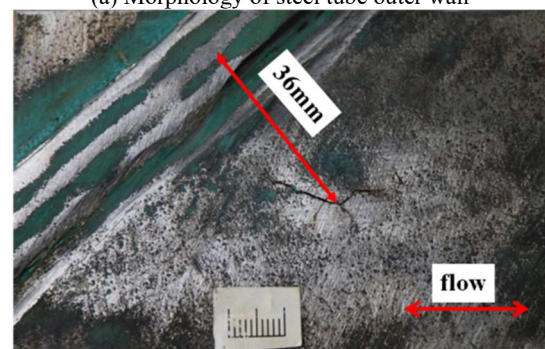
## 2 Macroscopic examination

The sample is the pipe section at the leakage site cut by a flame, and the leakage point is about one meter from the nearest pipe end. The morphology of the steel pipe after stripping the external coating is shown in Fig. 1. There are obvious cracks in the inner and outer walls of the steel pipe at the leakage point, and the cracks are distributed

along the longitudinal direction of the pipe body. The crack center is 36 mm away from the center of the spiral weld, as shown in Fig. 1(b).



(a) Morphology of steel tube outer wall



(b) Morphology of steel tube outer wall leakage point

**Fig 1.** Macroscopic appearance of leakage steel pipe

The Smartzoom5 super-depth digital microscope was used to observe the cracks at the leakage, and the results are shown in Fig 2. The length of the outer wall crack is 21 mm, and the length of the inner wall crack is 31 mm. Fig. 2 (b) shows that there is a pit in the inner wall of the

\* Corresponding author: xuyanxjtu@163.com.cn

steel pipe, 6 mm from the crack, and the maximum diameter is 2.4 mm. The wall thickness of the steel pipe near the crack was measured by ultrasonic thickness gauge. The wall thickness of the pipe at the pit was 5.9 mm, and that at other locations was about 7.1 mm.

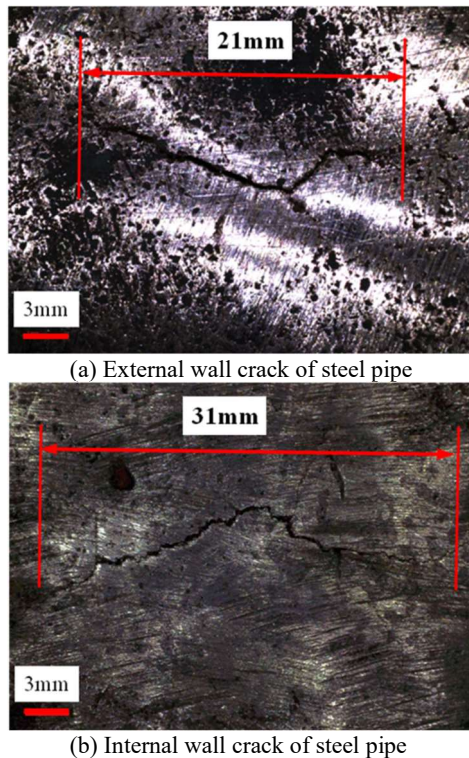


**Fig 2.** Macromorphology of cracks

### 3 Physical and chemical properties test

According to the standard requirements, chemical composition analysis, tensile properties, Charpy impact test, Vickers hardness test and metallographic examination were carried out on the pipe body of the steel pipe. All physical and chemical test samples were sampled at the position far from the defect.

#### 3.1 Chemical constituents analysis

The chemical composition analysis samples were taken from the tube far from the defect position, and the chemical composition was analyzed by using ARL 4460 direct-reading spectrometer according to ASTM A751-14a standard. The results are shown in Table 1.

**Table 1.** Chemical constituents (Wt×100%)

element	C	S	Mn	P	S	Cr	Mo	Ni	Cu
content	0.08	0.02	1.3	0.01	0.02	0.02	0.02	0.01	0.00
	5	3	8	1	6	9	2	6	4

#### 3.2 Mechanical properties test

Tensile properties, Charpy impact test and Vickers hardness test were carried out on the steel tube. The tensile strength is 563MPa and the yield strength is 453MPa. The Vickers hardness is 174~194HV10. When the test temperature was -20°C, the minimum absorption energy of the tube Charpy impact test was 232J, and the average was 266J. The above results meet the standard requirements.

#### 3.3 Metallographic analysis

The microstructure of the tube far from the defect position is shown in Fig. 3, which is ferrite and a small amount of pearlite. The grain size is 11.0, and there is no obvious abnormality.

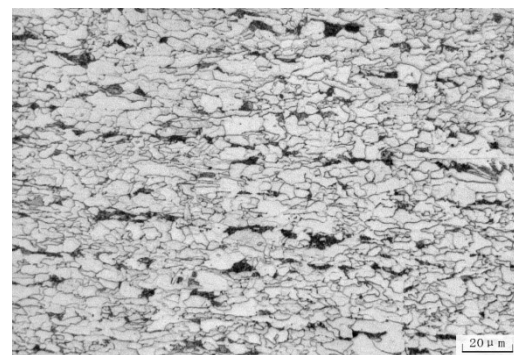


**Fig 3.** Tube structure away from leakage point

In order to understand the causes of cracks at the leakage of steel pipe, the T1 and T2 sections are intercepted along the direction perpendicular to the crack, as shown in Fig. 4. The full-thickness metallographic specimens are processed and observed by Smartzoom5 ultra-depth digital microscope and OLS 4100 laser confocal microscope.

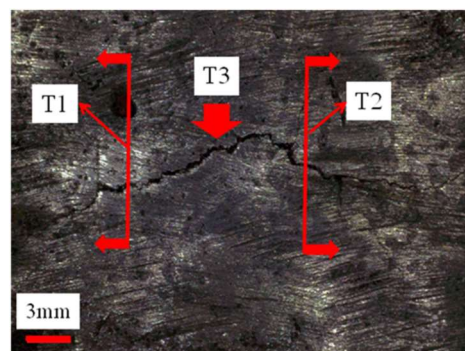


**Fig 4.** Sampling position of steel pipe leakage point

Fig 5 (a) is a photograph of the T1 section. The pit in the lower left corner corresponds to the inner wall pit found by the macroscopic inspection. The depth of the pit is about 1.2 mm, and the color of the pit and its adjacent cross section is abnormal, and the local color is purple yellow. The abnormal area is semi-elliptical, and the deepest part is close to the central position of the steel tube



wall thickness. There are holes at the interface between the color abnormal area and the tube matrix. The crack originates from the color abnormal area and extends to the outer wall. The microstructure at 1-1 is shown in Fig. 5 (b). The grains are abnormally coarse, and the color is different from the normal microstructure of the steel pipe, especially at the grain boundary. Fig. 5 (c) is 1-2 metallographic photographs. The grains near the main crack are coarse, the fine cracks propagate along the grain boundaries, and some purple inclusions exist in the grain boundaries.

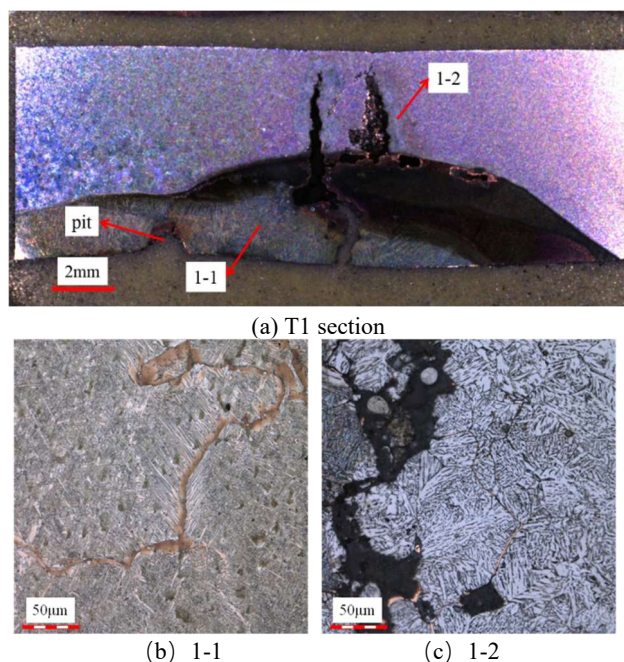


**Fig 5.** T1 section metallographic examination results

Fig. 6 (a) shows the photograph of T2 section, and there is still an abnormal area in the cross section of steel pipe. Fig 6 (b) is 2-1 metallographic photographs of the tube, which is located at the interface between the abnormal area and the normal tissue of the tube. The interface gap is obvious, and there are holes near the inner wall. The microstructure near the crack of the tube near the outer wall is overburned. Fig. 6 (c) in 2-2 metallographic photos, visible part of the grain boundary cracking, there are purple foreign bodies between grain boundaries, microstructure is overheating.

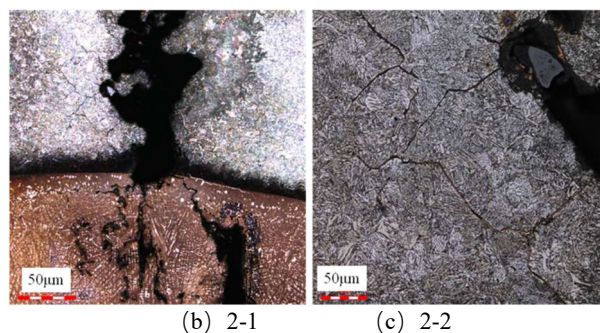
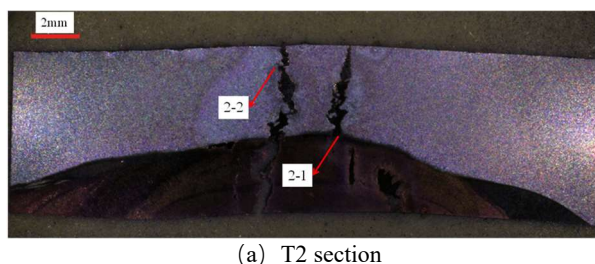


**Fig 6.** T2 section metallographic examination results

### 3.4 SEM micrograph and EDS analysis

The INCA 350 spectrometer was used to analyze the energy spectrum at different positions of the T1 section. The results are shown in Fig. 7. The main elements in the outer region are Fe, C and Mn, while the main elements in the inner color anomaly region are Fe, Cu and Mn. Among them, the copper element is abnormally high.

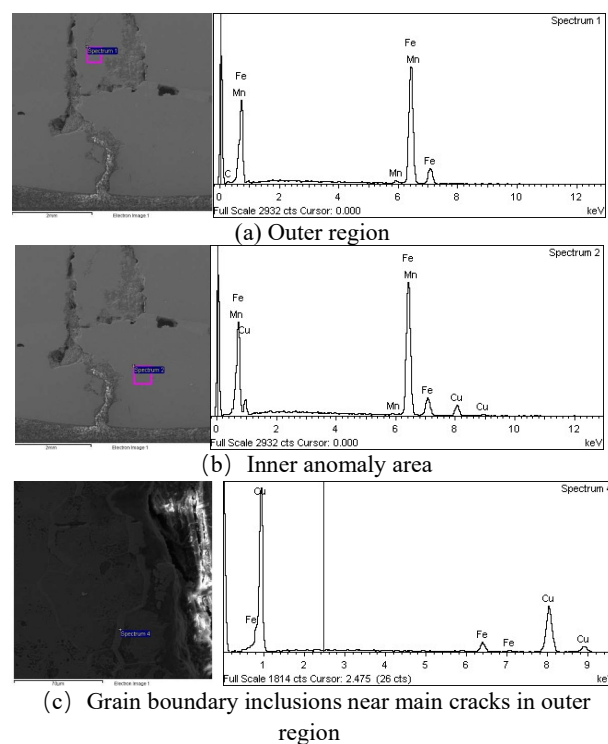


**Fig 7.** T1 section morphology and energy spectrum analysis

In order to better understand the distribution of Cu element, the T1 section and T2 section were analyzed by backscattered electron imaging. The results are shown in Fig 8. The contrast of backscattered electron imaging is caused by the difference in atomic number, so the distribution area of Cu element can be clearly distinguished. The area is consistent with the cross-sectional abnormal area found in metallographic observation, and it is semi-elliptical. In backscattered electron imaging, the contrast between the inner abnormal area and the outer tube interface area is higher, reflecting the higher content of Cu element.

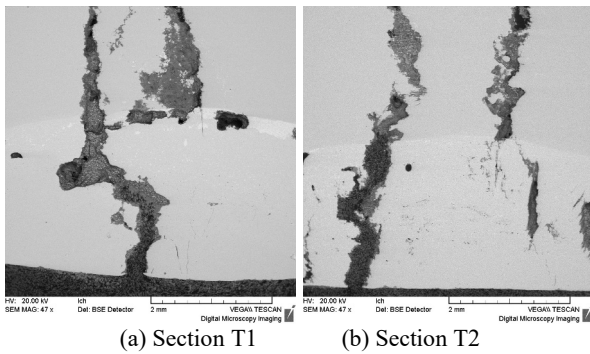


**Fig 8.** Backscattered electron imaging morphology

The cracks between T1 and T2 sections in Fig 7 were broken off, and the morphology of T3 fracture surface was observed, as shown in Fig 9. The fracture surface is obviously oxidized at high temperature. Fig 9 (a) is the fracture surface morphology of the inner layer, and Fig 9 (b) is the fracture surface morphology of the outer layer.

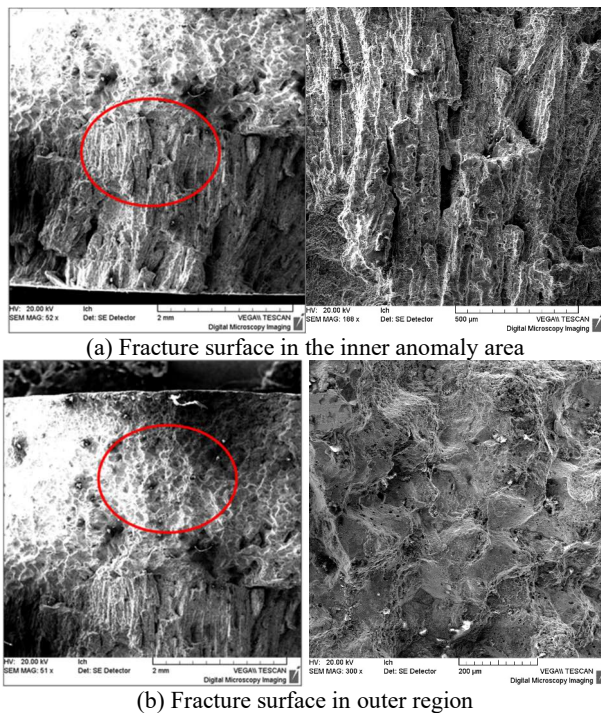
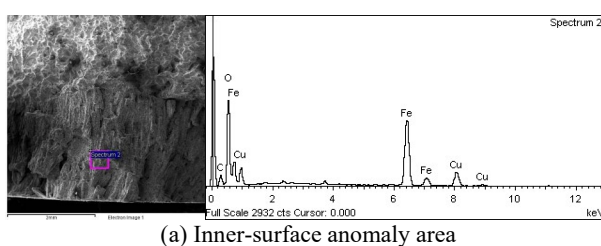
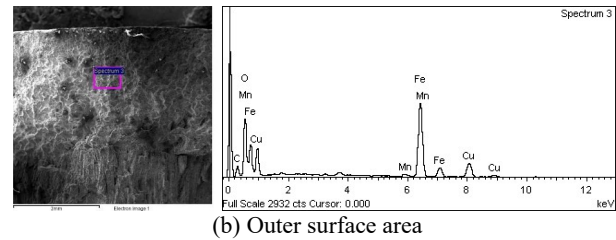


**Fig 9.** T3 Fracture Surface Morphology

The energy spectrum analysis of the inner and outer layers of the T3 fracture surface is carried out. The results are shown in Fig. 10. There are Cu elements in the abnormal area of the inner layer and the outer layer of the fracture surface, indicating that Cu elements are enriched in the crack area.



**(a)** Inner-surface anomaly area



**(b)** Outer surface area

**Fig 10.** T3 fracture surface energy spectrum analysis

## 4 Analysis and discussion

According to the product standard, the chemical composition, tensile test, Charpy impact test and Vickers hardness test results of the steel pipe body far from the leakage point are in line with the standard requirements. The metallographic structure is polygonal ferrite and a small amount of pearlite, and there is no abnormality. The macroscopic inspection results show that there are obvious cracks in the inner wall and outer wall of the steel pipe at the leakage, and the cracks are distributed along the longitudinal direction of the pipe body. The length of the inner wall crack is larger than that of the outer wall, and there is no obvious deformation of the pipe body at the leakage. The metallographic examination results show that the microstructure of the inner layer of the steel pipe at the leakage is abnormal, there are holes and pits, the grain is abnormally coarse, and the color is different from that of the normal pipe. The area is semi-elliptic and the deepest part is close to the center of the wall thickness, which is characterized by high temperature burn. The crack originated from the abnormal area in the inner layer of the steel pipe, expanded to the outer wall, and the fracture surface was obviously oxidized at high temperature. The microstructure near the main crack was coarse, and the fine cracks near the main crack extended along the grain boundary. There was Cu element enrichment in the crack gap.

The above results show that the main reason for the leakage of the steel pipe is that the leakage site experienced an abnormal high temperature process. When the working environment or heating temperature is abnormally increased, the low melting point metal Cu is melted into liquid, and part of the metal on the inner wall of the steel pipe is melted. The liquid Cu diffuses into the molten steel pipe matrix, resulting in abnormal Cu content in the inner layer of the pipe wall, and the color of the burning area is different from that of the normal part. However, part of the grain boundary of the steel pipe near the burnt part melts, and Cu diffuses along the grain boundary. The Cu element is enriched at the normal grain boundary, that is, the molten metal at the burnt part, the molten grain boundary and the crack jointly constitute the diffusion channel of Cu element, which further deteriorates the material strength and reduces the effective bearing capacity of the steel pipe. When the hydraulic test is carried out on the site, the crack propagates along the weak grain boundary, and finally leads to the leakage of the steel pipe.

It is generally believed [7,8] that when the actual working temperature of the part reaches about 2/3 or even

1/2 of the melting point temperature of the low melting point metal, under the action of tensile stress, the low melting point metal will infiltrate into the metal along the grain boundary to make it brittle, and gradually form cracks. When the low melting point metal is heated and liquefied, if it is directly contacted with the solid metal surface, the solid metal is often wet and brittle. Under the action of tensile stress, the crack starts from the surface, and the crack tip adsorbs low melting point liquid metal atoms, which further reduces the crystal bond strength of the solid metal and leads to the brittle propagation of the crack. In the absence of tensile stress and a certain temperature under the joint action will not produce low melting point metal contact embrittlement failure, tensile stress can be external tensile stress, can also be the residual stress formed in the process of parts.

According to the characteristics of high temperature burn and Cu pollution at the leakage site, it is speculated that the cause should be due to improper operation and contact between the grounding Cu electrode and the pipe body in the process of pipemaking or field pipeline laying. When the contact between the two is not good, the resistance becomes larger and the arc is generated. The high temperature arc leads to the burning of the pipe body and the melting of the Cu electrode, which leads to Cu pollution and cracking in the part.

## 5 Conclusions

The leakage of the steel pipe is mainly caused by the crack of the steel pipe caused by high temperature burning of the pipe wall and Cu pollution.

## References

1. Ning Mei, Sun Meihong, Zhong Shuming, et al. Analysis on Crack of High Pressure Air Bottle [J]. Tianjin Metallurgy, 2005(06):27-29+83.
2. Zhao Jun, Chen Yi, Chen Rong, et al. Failure Analysis on Copper Brittleness of Gas Cylinder [J]. Hot Working Technology, 2014,43(04):220-222.
3. Wang Gaofeng, Wu Jing, Nie Xianghui, et al. Cause Analysis of L415M LSAW Pipe Cracking [J]. Pressure Vessel Technology, 2016,33(07):58-62.
4. Xu Yan, Liu Yinglai, Nie Xianghui, et al. Research on Microstructures and Properties in Transition Zone of L415M Steel Grade Induction Heating Bending Pipe [J]. Hot Working Technology, 2016,45(16):175-178.
5. Wang Bin, Zhou Cui, Yang Li, et al. Cracking analysis of induction heating bended L415M pipeline steel [J]. Heat Treatment of Metals, 2013,38(08):123-127.
6. Xu Yan, Liu Yinglai, Nie Xianghui, et al. Prediction on the burst pressure of small diameter and thin wall steel pipe [J]. Oil & Gas Storage and Transportation, 2017,36(11):1265-1269.
7. Zhang Quanming, Chi Chun, Zhang Yong, et al. Study on Failure Cases of Liquid Metals Embrittlement [J]. Physics Examination and Testing, 2008(06):51-53.
8. Cao Xiaoyan, Li Tianlei, Luo Guangwen. Analysis on the Reasons Causing Cracks in Hot Bends [J]. Natural Gas and Oil, 2011,29(1):59-62.